Conceptual Design Report for the Multiple Disc Chopper Spectrometer at the Spallation Neutron Source

G. E. Granroth
Oak Ridge National Laboratory
March 25, 2001

Prepared for the Experimental Facilities Advisory Committee
SNS document IS-1.1.8.4-6043-RE-A-00

Table of Contents

1 Overview

An instrument with energy resolution that is variable between 10 and 100 μeV, over an incident energy (E_i) range of 2–20 meV, is a high priority of the Instrument Oversight Committee[1] (IOC) and the user community[2] of the Spallation Neutron Source (SNS). From the analysis described in this report, a Multiple Disc Chopper Spectrometer is the best instrument to cover this resolution range and will compliment the other inelastic instruments proposed for the Spallation Neutron Source. Specifically, the Multichopper spectrometer provides energy resolution and momentum transfer (Q) ranges complimentary to the Backscattering and Fermi chopper instruments planned for the SNS. Furthermore, it will have 2 orders of magnitude more flux on sample than existing disc chopper spectrometers.

The Multichopper instrument will include two pair of counter rotating high speed choppers separated by 35 m to provide, at the sample, a minimum time pulse width of 16 μs. This mode of operation is called the high intensity mode. A high resolution mode, that reduces the minimum pulse width to 8 μs at the expense of intensity, will also be available. The net result for the high intensity mode, observed in the detector bank located 5 m from the sample, is a minimum elastic energy resolution of 10 μeV for E_i = 2 meV. Furthermore this mode provides two orders of magnitude more flux on sample than existing disc chopper spectrometers[3,4,5] at equivalent resolutions. Detectors are located in a wide angle horizontal bank to provide a broad Q range and, at lower scattering angle, vertical banks to provide out of plane coverage. The out of plane detector coverage provides this instrument with unprecedented capabilities for the study of single crystal samples.

1.1 Instrument Performance

Figure 1 shows the energy transfer (ω) and Q space covered by the Multichopper spectrometer. A region assuming $E_i < 20$ meV is shown. The additional space covered if $E_i < 80$ meV is also shown. The ability to measure at $Q = 6$ Å^{-1} exceeds the request of the community[2] for this instrument. Furthermore, where this instrument's ω range overlaps with the Backscattering spectrometer, a greater range of Q is accessible with the Multichopper instrument. Where the Q range of the Multichopper and Fermi chopper instruments coincide, the Multichopper spectrometer provides finer energy resolution. Therefore, the ω-Q performance of the Multichopper spectrometer compliments the performance of other inelastic instruments that are planned for the SNS.

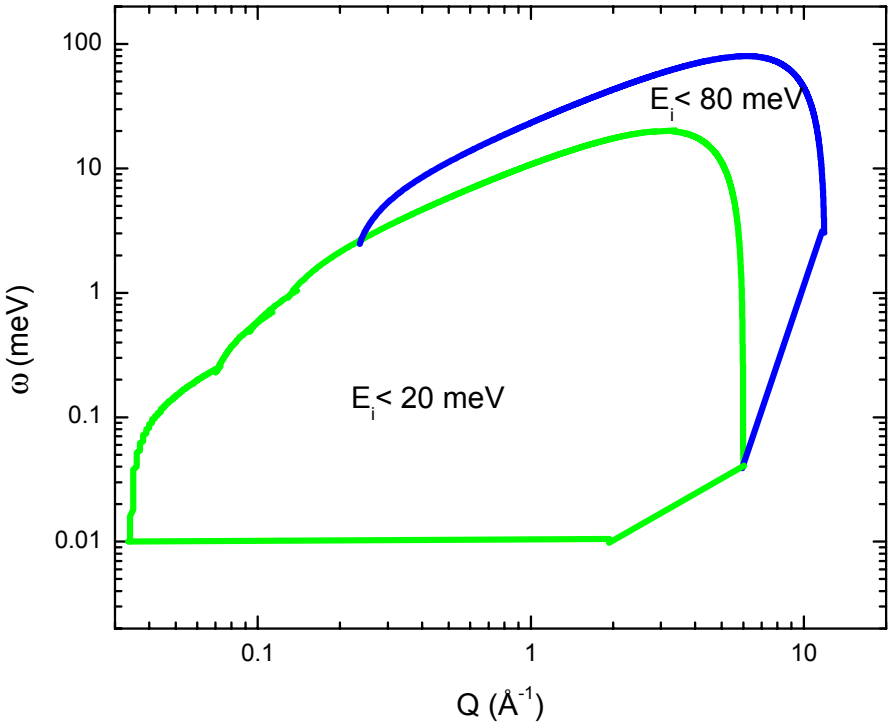

Figure 1 Energy transfer and Q space covered by the Multichopper spectrometer. The region covered by $E_i < 20$ meV is shown as well as an additional region for $E_i < 80$ meV.

Figure 2 shows the energy resolution ($\delta\omega$), at the elastic point, as a function of the incident energy over the design range. Both the high intensity mode and the added resolution range provided by the high resolution mode are indicated on the figure. The desired 10 μeV resolution is achieved for E_i = 2 meV in the high intensity mode. Additional flexibility to vary E_i and maintain a 10 μeV resolution is added by the use of the high resolution mode.

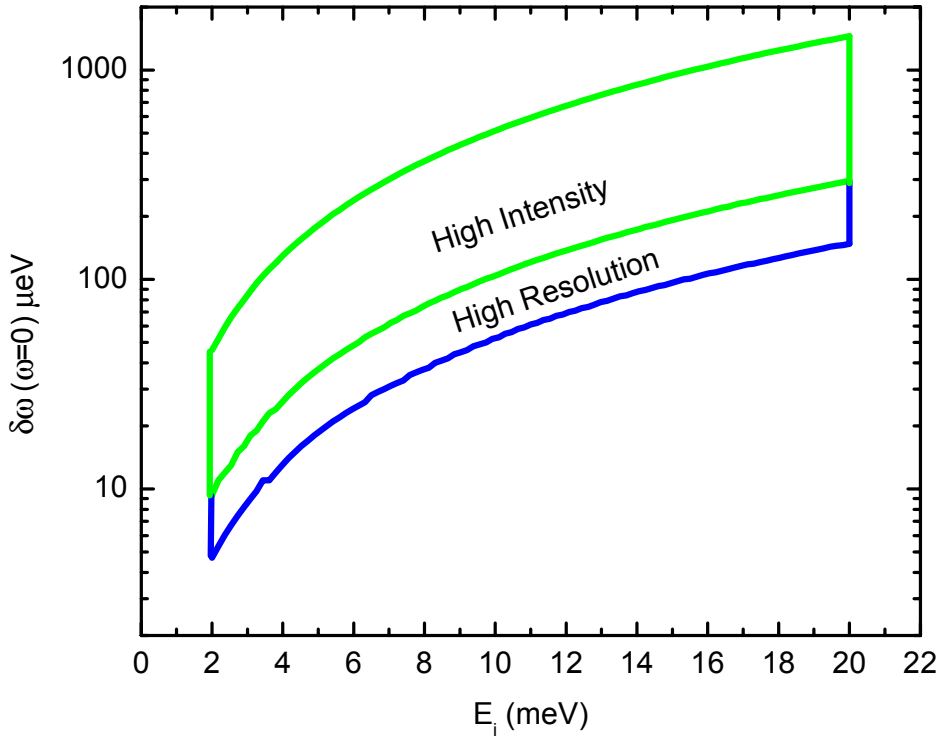

Figure 2 The energy resolution as a function of incident energy at the inelastic point. Note the high intensity and high resolution modes are distinguished from each other.

By reducing the chopper speed, resolution can be exchanged for intensity in a relatively continuous manner. For the high intensity mode, this change is shown in Figure 3. The edges of the colored region show $\delta\omega$ – E space similar to the high intensity mode in Figure 3 but extended to E_i = 80 meV. The color contours quantify the flux on sample for varying chopper speeds. This flux value is obtained by integrating over the time and energy window provided by the chopper system, at the sample postion, for each incident energy. Therefore it will be called the monochromatic flux on sample. For cases where even less resolution is required an additional chopper slit will be available to allow the user to gain even more flux by relaxing the resolution.

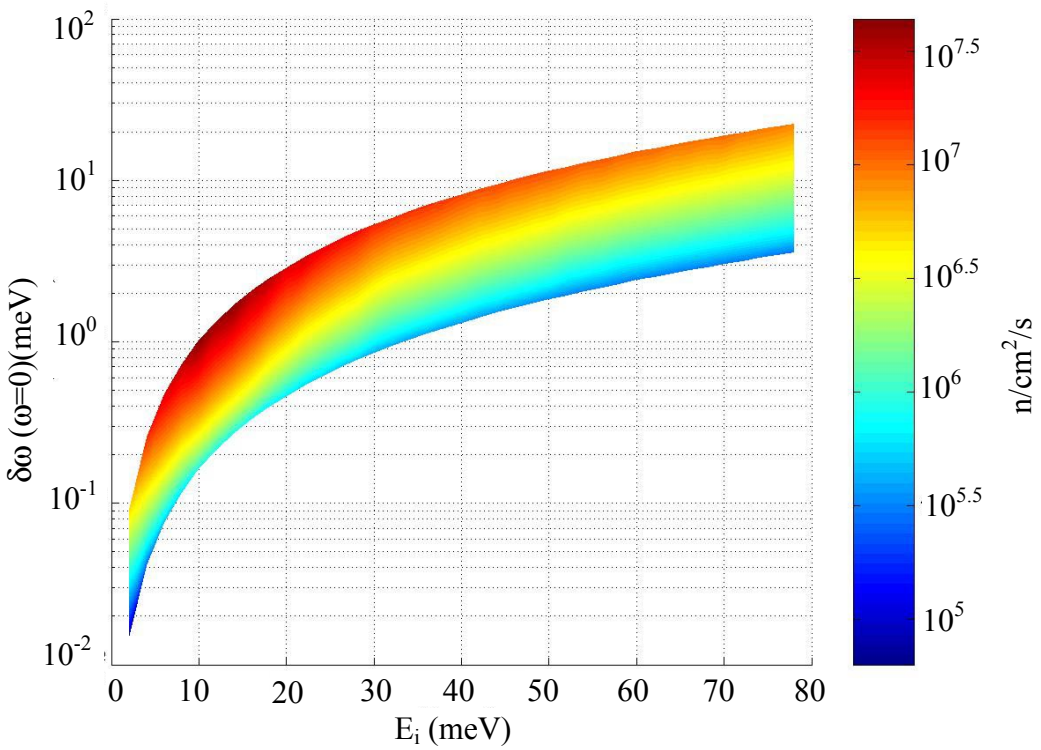

Figure 3 Resolution as a function of incident energy for high intensity mode over the full range of E_i. The color spectrum represents the flux on sample for different E_i and $\delta\omega$ combinations.

1.2 Instrument Description

Figure 4 shows a three dimensional view of the Multichopper spectrometer with the components labeled according to Table 1.

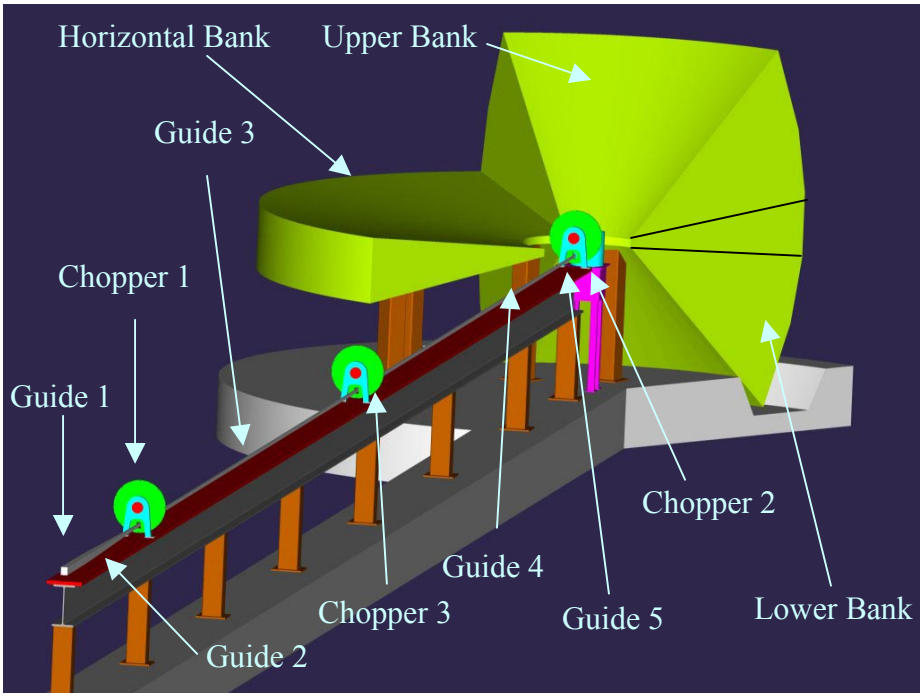

Figure 4 Three dimensional rendered view looking down the guide of the Multichopper spectrometer. The components are labeled according to the scheme in Table 1

After leaving the moderator, the neutron beam is funneled (Guide 2) down to a width of 3 cm so a pair of counter rotating choppers (Chopper 1) running at 300 Hz can provide a 32 μs time pulse. The curved guide (Guide 3) ensures that line of sight to the moderator ends at 31 m away from the moderator. The straight section of guide (Guide 4) brings the peak flux in the neutron beam back to the center of the beam. Finally the second funnel (Guide 5) reduces the beam width to 1.5 cm so another pair of counter rotating choppers (Chopper 2) running at 300 Hz can provide a 16 μs time pulse. Chopper 3 eliminates second order contamination and does not need to run faster than the repetition rate of the source. However, neutron energy gain scattering can interfere with neutron energy loss scattering from an adjacent frame for low E_i. To avoid this frame overlap, this chopper will be run at 30 Hz for $\omega > 0.8xE_i$ when $E_i < 5$ meV are required.

Table 1 Mutltichopper spectrometer parameters

Component	Parameter	Value
Source	Moderator	Liquid H_2, coupled, Beam line 5
Primary Spectrometer		
Distances	Moderator-chopper 1 Chopper 1-chopper 2	6 m 35 m

	Chopper 2 -sample	1 m
Chopper1	Type Radius from beam center Frequency # of slots Slot sizes (h x v) Distance from moderator	Counter rotating dual disk 25 cm Variable 60-300 Hz 3 10 cm x 1.5 cm, 3 cm, 6 cm 6 m
Chopper2	Type Radius from beam center Frequency # of slots Slot sizes (h x v) Distance from moderator	Counter rotating dual disk 25 cm Variable 60-300 Hz 3 10 cm x 0.75 cm, 1.5 cm, 3 cm 41 m
Chopper 3	Type Radius from beam center Frequency # of slots Slot size (h x v) Distance from moderator	Disk 25 cm Variable 30-60 Hz 3 10 cm x 3 cm 11 m
Guide 1	Type Coating Dimensions (h x v) Length	Straight 3 x θ_c^{Ni} Supermirror 12 cm x 10 cm 1 m
Guide 2	Type Coating Entrance dimensions (h x v) Exit dimensions (h x v) Length	Funnel 3 x θ_c^{Ni} Supermirror 12 cm x 10 cm 10 cm x 3 cm 5 m
Guide 3	Type Coating Dimensions (h x v) Curvature Length	Curved 2 x θ_c^{Ni} Supermirror 10 cm x 3cm 2.1 km 25m
Guide 4	Type Coating Dimensions (h x v) Length	Straight 2 x θ_c^{Ni} Supermirror 10 cm x 3cm 5 m
Guide 5	Type Coating Entrance dimensions (h x v) Exit dimensions (h x v) Length	Funnel 3 x θ_c^{Ni} Supermirror 10 cm x 3 cm 10 cm x 1.5 cm 5 m
Secondary Spectrometer		
Distance	Sample-detector distance	5 m

Detectors	Type Pressure Dimensions (h x v)	He^3 PSD 8 Atm 100 cm x 2.54 cm
Horizontal Bank	Horizontal angular coverage Vertical angular coverage # of detectors	-30^o – -1.5^o, 1.5^o – 150^o -5^o – -1.5^o, 1.5^o – 5^o 620
Upper Bank	Horizontal angular coverage Vertical angular coverage # of detectors	-30^o – 30^o 5^o – 30^o 414
Lower Bank	Horizontal angular coverage Vertical angular coverage # of detectors	-30^o – 30^o -5^o – -30^o 414

2 Instrument Design

There are several proposed designs for a 10-100 μeV spectrometer. Section 2.1 will describe each design and explain their capabilities and limitations. This discussion will illuminate why the Multichopper spectrometer is the design of choice. Section 2.2 will provide a detailed description of the selected concept.

2.1 Spectrometer choice

Three different designs of spectrometer have been proposed to meet the energy resolution requirement of 10-100 μeV. Two of these designs, the Multichopper spectrometer and a crystal monochromator instrument, are direct geometry machines. The third design is a crystal analyzer spectrometer; an inverse geometry design. To compare the merits of each type of instrument, the resolution and monochromatic flux on sample are compared.

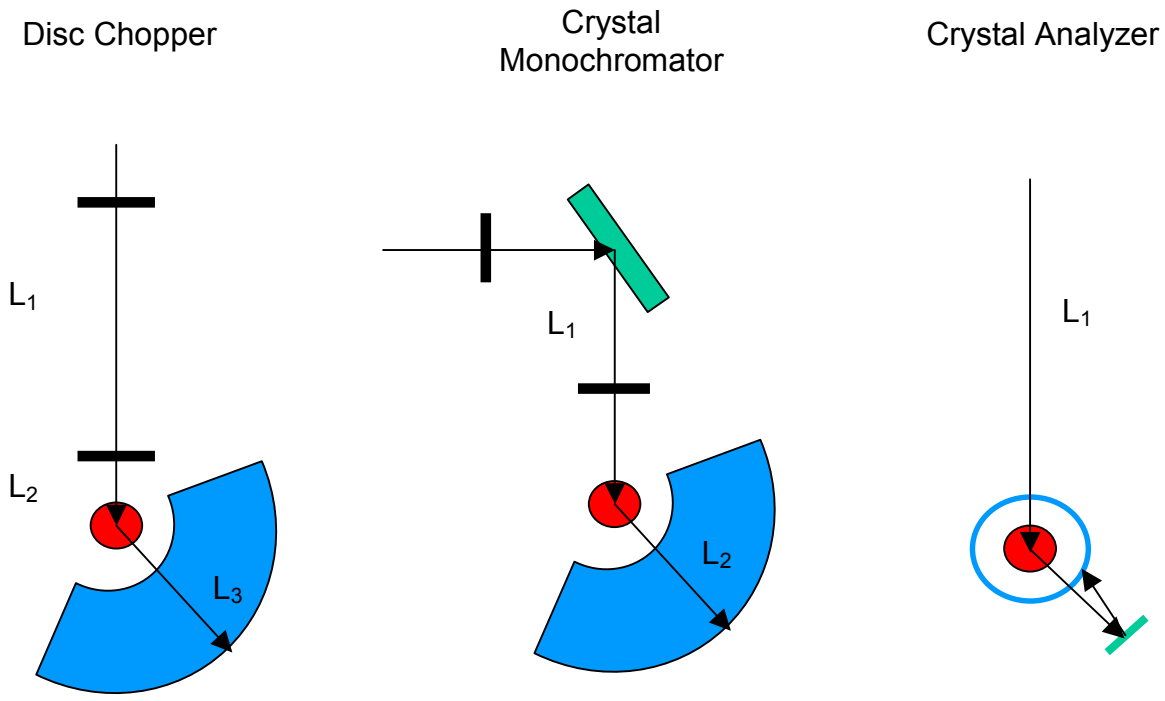

Figure 5 Schematic diagrams for Multichopper, crystal monochromator, and crystal analyzer designs. The labeled distances are used in the resolution calculations. The heavy dark lines indicate choppers. For the crystal monochromator instrument, two potential chopper locations are available to increase resolution.

Figure 5 shows schematic diagrams for the Multichopper, a crystal monochromator, and crystal analyzer spectrometers. Only the components needed for calculation of the energy resolution and the monochromatic flux on sample are shown. Samples are in red, detectors are in blue, crystals are in green, and dark heavy lines are choppers. First the crystal monochromator instrument will be compared with the Multichopper spectrometer. After that, the crystal analyzer spectrometer will be compared with the Multichopper spectrometer.

The energy resolution for the Multichopper instrument is given by:

$$\delta\omega = m_n\left[\left(\frac{v_i^3}{L_1}+\frac{v_f^3 L_2}{L_1 L_3}\right)^2\delta t_m^2+\left(\frac{v_i^3}{L_1}+\frac{v_f^3\left(L_2+L_1\right)}{L_1 L_3}\right)^2\delta t_c^2+\left(\frac{v_f^3}{L_3}\right)^2\delta t_d^2\right]^{\frac{1}{2}} \quad (1)$$

where m_n is the mass of the neutron, v_i and v_f are the initial and final velocities of the neutrons, respectively, L_1, L_2, and L_3 are the distances defined in Figure 2, δt_m is the time width of the first chopper, δt_c is the time width of the second chopper, and δt_d is an uncertainty in the final flight path associated with things like uncertainty of position of detection in the detector, sample size, and detector size. Actually Equation (1) is for the case of a single chopper instrument[6,7]. However for resolution purposes, the Multichopper instrument can be considered a single chopper instrument with the time width of the moderator defined by the first chopper. To optimize the Multichopper instrument for resolution, L_1 and L_3 need to be maximized since they are in the denominator. Furthermore L_2 should be minimized since it is in the numerator. Therefore the Multichopper instrument is best optimized for resolution as a long instrument.

The energy resolution for a crystal monochromator instrument is given by[7]:

$$\delta\omega = 2E_i\left\{\left[\cot(\theta)\left(1+\frac{L_1}{L_2}\left(1-\frac{\omega}{E_i}\right)^{\frac{3}{2}}\right)\right]^2\delta\theta^2+\left[\left(1-\frac{\omega}{E_i}\right)\frac{\delta t_m}{t_2}\right]^2\right\}^{\frac{1}{2}} \quad (2)$$

where E_i is the incident energy, ω is the energy transferred, θ is the Bragg angle, L_1, and L_2, are the distances defined in Figure 2, t_2 is the time to travel the distance L_2, $\delta\theta$ is the mosaic of the monochromator crystal and δt_m is the time width of the moderator. To reduce the effective time width of the moderator, a chopper can be introduced before the monochromator as shown in Figure 2. For this instrument L_1 is in the numerator and L_2 is in the denominator. Therefore a crystal monochromator instrument optimized for resolution is a relatively short instrument. However if a chopper is introduced into the system, the important quantity is the distance between the chopper and the monochromator and the length of the instrument is less important. For the case of the

chopper before the monochromator, L_1 can simply be replaced by the distance between the chopper and the monochromator. The case for the chopper after the monochromator is only slightly more involved. Basically a monochromator removes the moderator dispersive component from the resolution function[7]. This means that a chopper after the mononchromator can be modeled by a chopper before the monochromator with a time window of,

$$\delta t_{eff} = \frac{\delta t_m}{\left(1 + \frac{L_c}{L_1}\right)}, \quad (3)$$

where δt_m is the time width of the chopper, L_1 is the distance between the effective chopper and the monochromator and L_c is the distance between the monochromator and the real chopper position. Therefore the resolution is calculated by substituting δt_{eff} for δt_m in equation (2).

Since both the Multichopper and crystal monochromator spectrometers are direct geometry instruments, a complete resolution comparison can be performed at the elastic point.

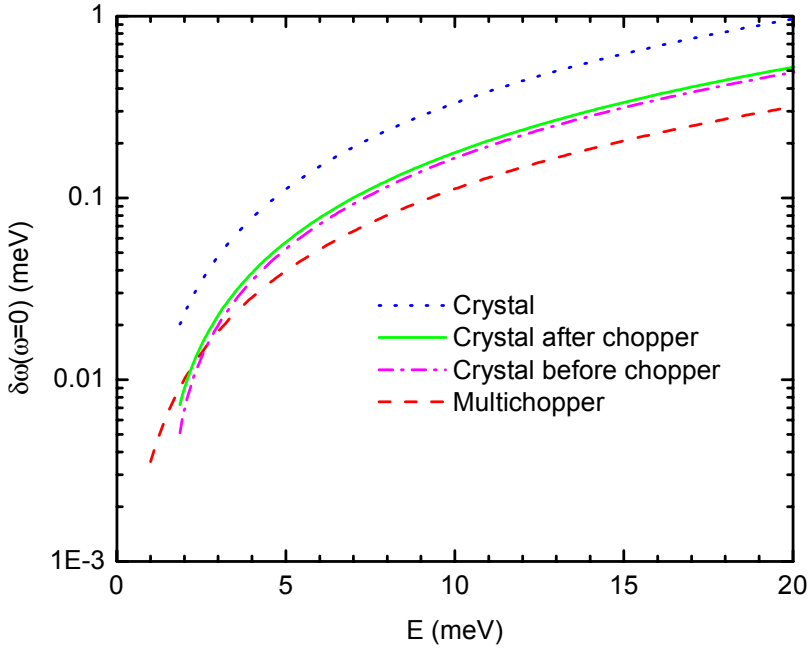

Figure 6 Energy resolution at the elastic point vs. incident energy for a crystal monochromator instrument, crystal monochromator instrument with choppers before and after the monochromator, and the Multichopper instrument. The parameters for each instrument are provided in the text.

Figure 6 shows the energy resolution vs. incident energy for the crystal monochromator instruments (both with and without choppers) and the Multichopper spectrometer. For the Multichopper spectrometer $L_1 = 30$ m, $L_2 = 1$ m, $L_3 = 5$ m, $\delta t_m = 32$ µs, and $\delta t_c = 16$ µs. The crystal monochromator resolution was calculated under the assumption that a

PG(002) monochromator was used with $\delta\theta = 10'$, $L_1 = 5$ m and $L_2 = 5$ m for the case with no choppers. For both cases with choppers, $L_1 = 2$ m and for the case with the chopper after the monochromator $L_c = 1$ m. The configuration without a chopper provides $\delta t_m =$ 45 μs and for the cases with a chopper $\delta t_m = 16$ μs is used. From a resolution standpoint a crystal monochromator instrument with a fast chopper can provide finer resolution than a Multichopper spectrometer for $E_i < 2$ meV. In all other cases the Multichopper spectrometer provides finer resolution.

For an intensity comparison the crystal monochormator with a chopper after the monochromator was used. This configuration not only provides the best resolution, but also will have the most flux on sample since there is no beam compression only for the chopper. Fermi choppers are typically used in this application[8,9]. For comparison of an optimized crystal monochromator-Fermi chopper instrument with the Multichopper instrument, two virtual instrument primary flight paths have been set up in the Monte Carlo simulation program MCSTAS[10]. The crystal monochromator-Fermi chopper instrument consists of 35 m of a 10 cm x 12 cm guide that ends 1 m before a vertically focusing PG(002) monochromator with 80% reflectivity. The monochromator focuses the beam through a Fermi chopper 1 m away to a sample 2 m from the monochromator crystal. For each E_i studied, the Fermi chopper slit package was optimized for the corresponding neutron velocity. The time width of the pulse on the sample was 16 μs, which is consistent with the analytical calculations presented above. The Multichopper model that was used is described by the parameters in Table 1 and the choppers were operated to produce a 16 μs pulse width on the sample. A 5 cm high x 1.5 cm wide sample (#1) was tested as well as a 5 cm high x 12 cm wide sample (#2). The results are shown in Figure 7. For the smaller sample, the Multichopper instrument clearly outperforms the crystal monochromator instrument. However when the full beam is taken into account (sample #2), the intensity on the sample is comparable for both designs. The differences for the smaller sample arise from the fact that the beam for the Multichopper spectrometer is both horizontally and vertically compressed, where the crystal monochromator instrument is only vertically focused. Therefore, a double focusing crystal monochromator-Fermi chopper instrument is likely to provide equivalent performance to the Multichopper machine. However the crystal monochromator machine would require moving a large detector bank and thus the performance of the instrument would be limited by space constraints. One potential benefit of a crystal monochromator-Fermi chopper instrument is that horizontal focusing would allow the size of the Fermi chopper to be decreased. The net result would be a smaller time pulse on the sample. Then, in principal, the final flight path could be shortened to produce the same energy resolution. However section 2.2.4 will show that for shorter flight paths squashed PSD ^{3}He tubes are essential and they are currently not available. In summary, a crystal monochromator-Fermi chopper machine could in principal perform in an equivalent manner to a Multichopper spectrometer. However the Multichopper design is favored for technical design reasons.

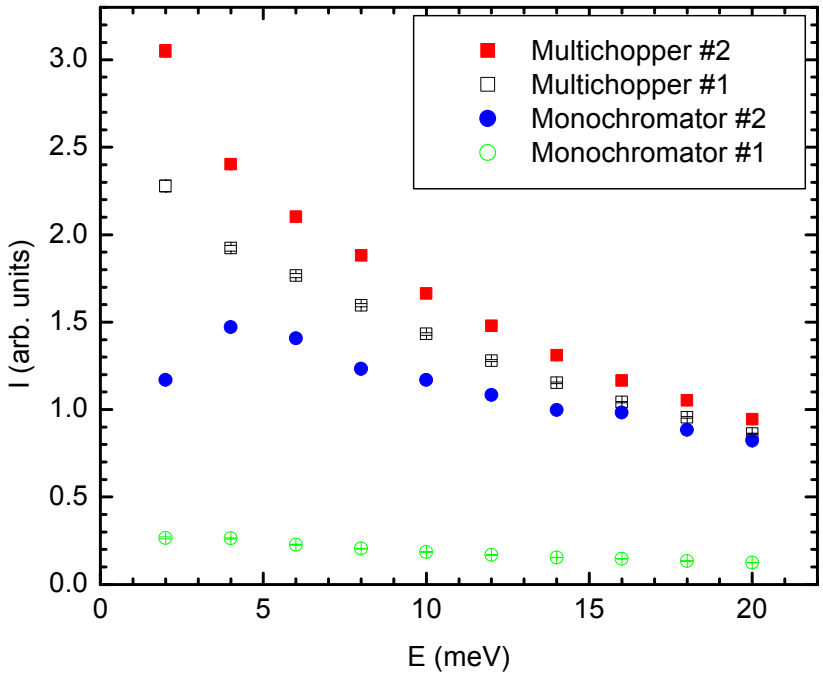

Figure 7 Intensity on a 5 cm x 1.5 cm sample (#1) and a sample the full width of the beam (#2) vs. incident energy for the Multichopper spectrometer and a crystal monochromator-Fermi chopper instrument.

Following the design of the SNS Backscattering Spectrometer[11], the energy resolution of a crystal analyzer spectrometer is given by the following equations. First for the primary spectrometer,

$$\delta\omega_p = 2E_i \frac{\delta t_m}{t_1} \quad (4)$$

where E_i is the incident energy, t_1 is the time to travel a distance L_1, and δt_m is the time width provided by the moderator. For the secondary spectrometer,

$$\delta\omega_s = 2\left[E_i^2\left(\frac{\delta t_f}{t_1}\right)^2 + E_f^2\left(\left(\frac{\delta d}{d}\right)^2 + (\cot(\theta)\delta\theta)^2\right)\right]^{\frac{1}{2}} \quad (5)$$

where E_f is the final energy, d is the atomic spacing of the crystal, θ is the Bragg angle of the analyzer crystal, δt_f is the uncertainty in the time at the detector, δd is the uncertainty in the atomic spacing, and δθ is the mosaic of the analyzer crystals. The total resolution of the crystal analyzer instrument is then given by,

$$\delta\omega = \sqrt{\delta\omega_s^2 + \delta\omega_p^2}\,. \quad (6)$$

The resolution for the Multichopper spectrometer is provided by Equation (1). Since the back scattering instrument is an inverse geometry instrument and the Multichopper spectrometer is a

direct geometry instrument, the best comparison is to examine the δω vs. ω for several different crystal analyzer spectrometers and the Multichopper spectrometer with several different values of E_i.

Figure 8 shows the aforementioned plot.

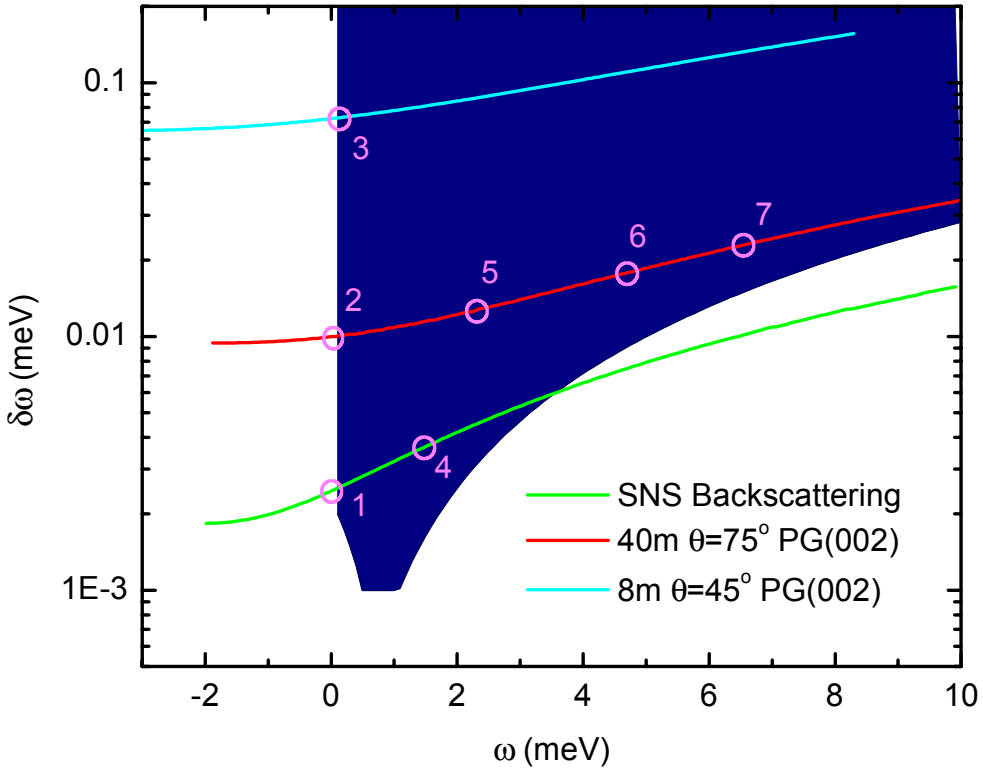

Figure 8 Resolution vs. energy transfer for the Multichopper spectrometer and three different crystal analyzer spectrometers. The region indicates the range covered by the Multichopper spectrometer and the curves represent the three crystal analyzer spectrometers. The circles indicate points where comparisons of the monochromatic flux on sample have been made in Table 2.

The continuous region is the space covered by the Multichopper spectrometer for various E_i and chopper speeds. The bottom curve represents the SNS Backscattering spectrometer. The middle curve is for a shorter crystal analyzer spectrometer with PG(002) analyzer crystals set for a 75° scattering angle. This particular instrument is most directly comparable to the highest resolution modes of the Multichopper spectrometer. The light blue curve is for an even lower resolution crystal analyzer instrument. Note that to cover the same range of δω and ω three crystal analyzer instruments are needed where only one Multichopper spectrometer is needed. Furthermore the Multichopper spectrometer provides better resolution at large energy transfers where the crystal analyzer instrument provides better resolution near the elastic point.

A comparison of the flux on sample for these two instrument types needs to be made. Since crystal analyzer instruments have a white incoming beam, the definition of monochromatic flux on sample needs to be modified for this instrument. Instead of a chopper defining the time and energy width, the analyzers define this time and energy

width. Since most neutrons hit the sample but are not reflected into the detector by the analyzer crystals, the monochromatic flux on sample is defined by integrating over this analyzer defined time and energy window at the sample position. Furthermore, the crystal analyzer instruments are fixed E_f machines and the Multichopper instrument is a fixed E_u machine. Therefore comparisons must be made at equivalent energy transfers. Now with appropriate analysis method and definitions for the monochromatic flux on sample, a direct intensity comparison can be made. Several points of equivalent $\delta\omega$ and ω were chosen at which to compare flux and are indicated by the circles in Figure 8. The fluxes are summarized in Table 2. For the elastic points, crystal analyzer instruments usually win by about an order of magnitude in flux. However for points like number 3, where several different values of E_i can be used in combination with different chopper speeds to obtain the same ω and $\delta\omega$ point, Q range can be sacrificed for intensity with the Multichopper spectrometer and then, with E_i = 2 meV, the two spectrometer types have a nearly equivalent flux. Examination of inelastic points 4-7 shows that the fluxes are comparable for points 4 and 5 and that the Multichopper spectrometer puts more flux on sample for points 6 and 7.

Table 2 Flux comparisons between crystal analyzer spectrometers and a Multichopper spectrometer. The point number corresponds to the circles in Figure 8.

	Multichopper spectrometer				Crystal analyzer spectrometers	
Point	E_i (meV)	Chopper ν (Hz)	n/cm²/s	Max Q (Å^{-1})	n/cm²/s	Max Q (Å^{-1})
1	0.8	600	1.0×10^{4}	1.7	1.0×10^{5}	2.7
2	2	600	6.3×10^{4}	2.7	4.7×10^{5}	2.7
3	7.5 6 4 2	600 420 240 180	5.3×10^{5} 8.6×10^{5} 1.3×10^{6} 2.3×10^{6}	5.2 4.6 3.8 2.7	3.2×10^{6}	3.7
4	2	600	6.3×10^{4}		8.8×10^{4}	
5	4	600	2.3×10^{5}		3.6×10^{5}	
6	6	600	4.2×10^{5}		2.4×10^{5}	
7	7.5	600	5.3×10^{5}		1.7×10^{5}	

Furthermore, if a lower resolution crystal analyzer spectrometer were to be built instead of the Multichopper spectrometer, the one represented by the red curve in Figure 8 would be the one to build. Then only points 2 and 5 – 7 are directly comparable. Second, the Multichopper spectrometer has finer Q resolution than a crystal analyzer spectrometer. The gain obtained by relaxing the Q resolution (grouping detectors) for the Multichopper spectrometer has not been included in the above calculations, but would roughly increase the detected flux by a factor of 2.

In conclusion, crystal analyzer and crystal monochromator spectrometer designs have been compared to the Multichopper spectrometer design. The flexibility of the

Multichopper instrument, as compared to the other potential designs, makes it the best choice for the 10 – 100 μeV spectrometer.

2.2 Multichopper design

The following sections describe the analysis that has gone into the conceptual design of the instrument. The instrument was optimized for an energy range between 2-20 meV. Nevertheless, there are several instances where the instrument design allows for use outside of this regime and these regions will be noted.

2.2.1 Moderator Choice

A cursory look at the different moderators for the Multichopper spectrometer shows that a T = 20 K liquid H_2 moderator is the best choice for the 2 – 20 meV energy range. However, a more detailed discussion is required to choose between the coupled (beam 5) and decoupled (beam 2). A detailed study shows that the quantity of importance for the highest resolution modes is the peak flux as a function of energy. Since the choppers select such a short pulse, the time width of the emitted pulse is inconsequential. Figure 9 shows the peak flux emitted from the coupled and decoupled liquid H_2 moderators.

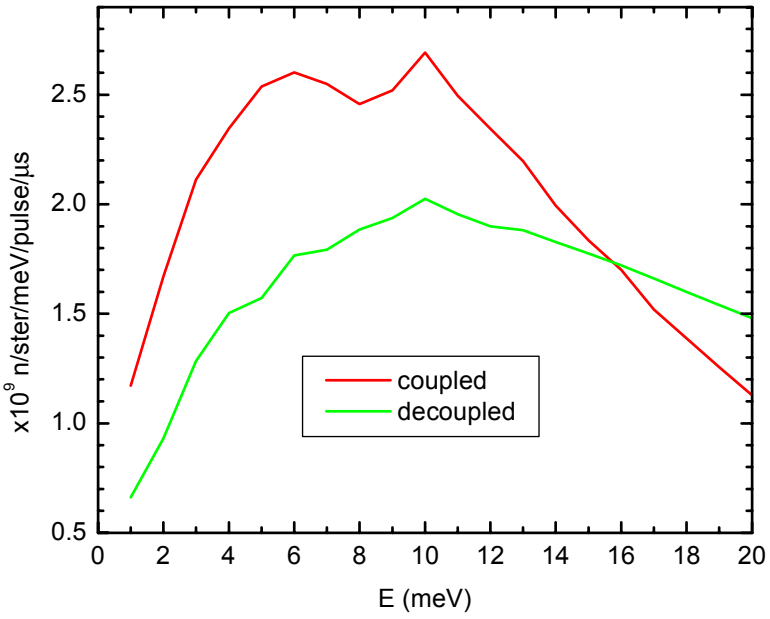

Figure 9 Peak flux emitted by the coupled and decoupled liquid H_2 moderators.

For most of the design range of E = 2 - 20 meV the coupled moderator is the better choice. Furthermore when choppers are slowed down to decrease the resolution and increase intensity, the additional flux in the tail of the coupled moderator can be useful and then the coupled moderator is better for the full energy range.

2.2.2 Guide Design

The guide design can be broken down into three components: design of the funnels, design of the curved section, and overall length considerations. Besides compressing the beam down to the size of the sample, the funnels also squeeze the beam to a width such that a 32 μs pulse can be produced at the first chopper and a 16 μs pulse can be produced at the second chopper. This requirement means that the first funnel must bring the guide down to a width of 3 cm and the final funnel must reduce the guide width to 1.5 cm.

The primary design constraint on the curved guide was for the flight path to leave line of sight before exiting the building. This constraint arises from the cost of the floor in external buildings to hold the weight of shielding required for beamlines before line of sight is reached. Two approaches have been considered to deal with this restriction: first, a guide with a 2.6 km curvature, and second a 3 channel bender with a 270 m radius of curvature. The curved guide was modeled as 25, 1 m long sections and the bender was broken into 16, 0.5 m segments. Both components were simulated assuming m = 3 supermirror with reflectivities and cutoffs taken from fits to measured data. Figure 10 shows the guide gains and a comparison for the two configurations.

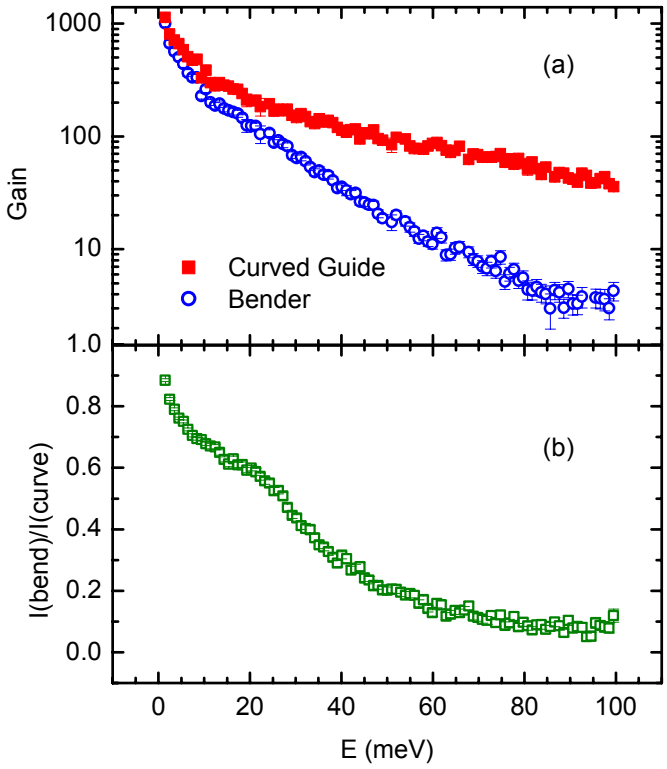

Figure 10 Guide gain of curved guide vs. bender. (a) guide gain as compared to no guide and a 1.5 cm wide by 5 cm high sample. (b) ratio of guide gain of bender as compared to curved guide.

Guide gain is measured with respect to natural illumination of the sample. Figure 10a shows that, for the curved guide, gains of better than 100 are obtained for $E_i < 60$ meV. The bender does not perform as well and its loss of performance is dramatically shown in Figure 10b. Notice for $E_i = 2$-20 meV, the bender puts 20-40% less neutrons on sample than the curved guide. Therefore the curved guide is favored in the current design.

The final consideration is the total length of the guide. Inorder to produce 10 μeV resolution with $E_i = 2$ meV neutrons, the distance between the two choppers should be 35 m. Furthermore, iterative Monte Carlo simulations – using Mcstas[10] – have shown that 5 m funnels provide the highest flux on sample when coupled with the curved guides. In addition, a 5 m straight section is needed after the curve to randomize the resultant flux distribution so the peak flux is in the center of the beam. With all these components assembled, Figure 11 shows a scaled view of the total guide design. Notice that the guide leaves line of sight just before 30 m, the location of the target building wall. Further guide optimizations and considerations are in progress and are described in section 3.

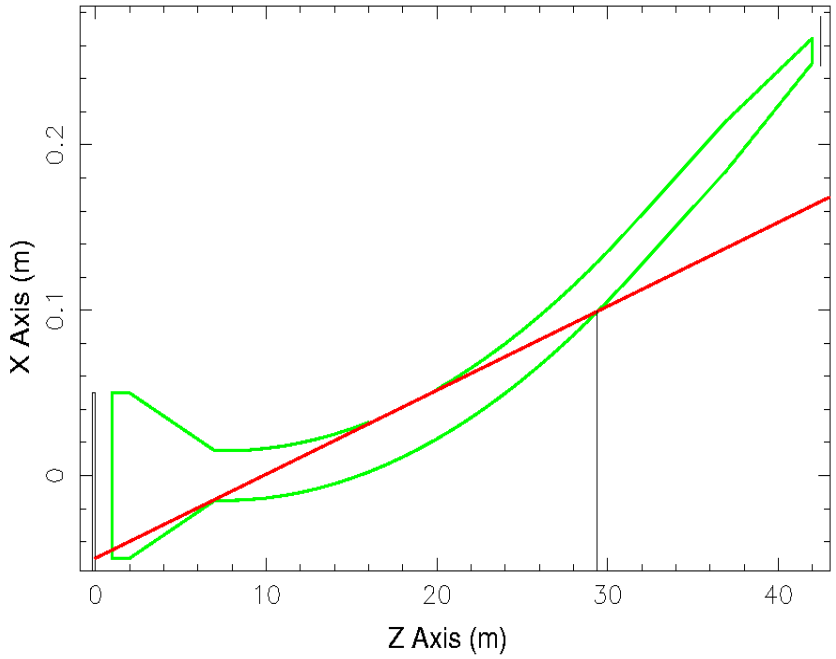

Figure 11 Scaled view of guide. Notice the guide leaves line of sight just inside 30 m, the edge of the target building.

2.2.3 Chopper design

As was mentioned in Section 2.2.2, the first and last choppers should be placed 35 m from each other to meet the resolution requirements. This requirement also means that counter rotating dual disk choppers with a maximum speed of 300 Hz per disc will be used. An additional chopper will be needed for frame overlap and second order suppression. This chopper will be a standard single disc bandwidth chopper that runs at

60 Hz. It also needs to be able to run at 30 Hz for cases where frame overlap is a potential problem.

The optimal position for this chopper can be determined by examination of the timing diagram for the spectrometer shown in Figure 12. This figure includes the 3 choppers, 2 frames of E_i = 2 meV neutrons, the location of the sample and detectors and a line indicating the highest energy neutrons that are not filtered out by the guide. Assuming that neutrons of E_i > 80 meV are filtered out, chopper 3 can be no farther away than 12 m from the moderator. If it is placed farther away, neutrons of $E_i < E < 80$ meV will also be in the guide system causing an elevated background. For most values of E_i and ω, frame overlap is not a concern for this instrument, but for E_i < 5 meV and $\omega > 7/8E_i$ it is. Figure 12 shows a case of frame overlap for E_i = 2 meV. Figure 13 shows a closer view of the region where frame overlap is a problem.

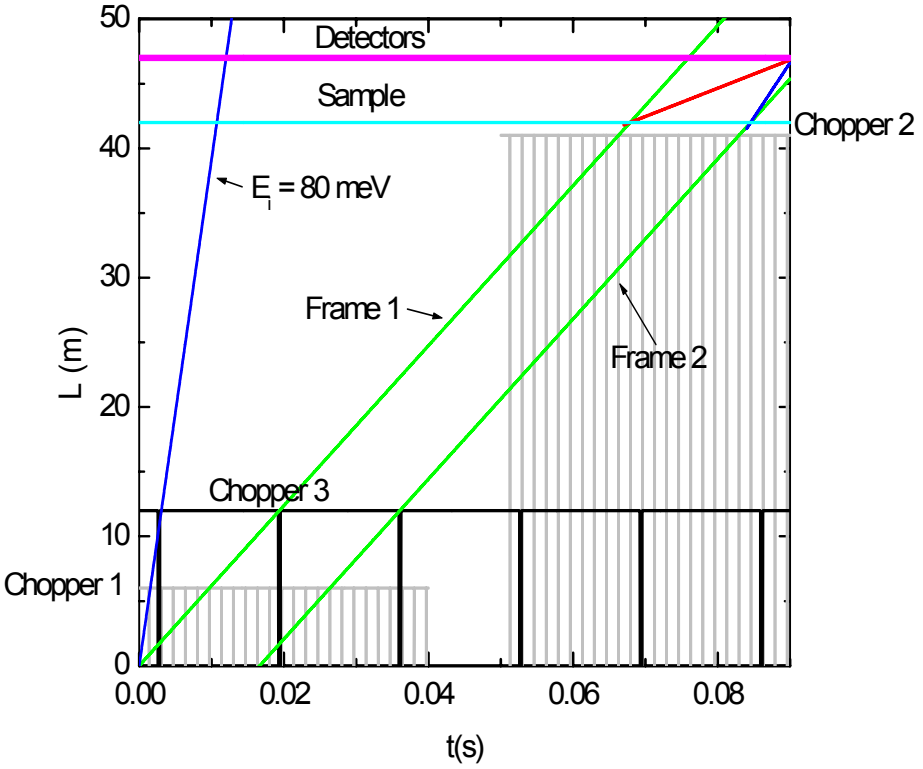

Figure 12 Timing diagram for the Multichopper spectrometer. For choppers 1 and 2 only two frames worth of chopper open times are shown for clarity. A high energy cutoff and a condition for frame overlap are also shown. The neutrons shown to hit the sample are E_i = 2 meV.

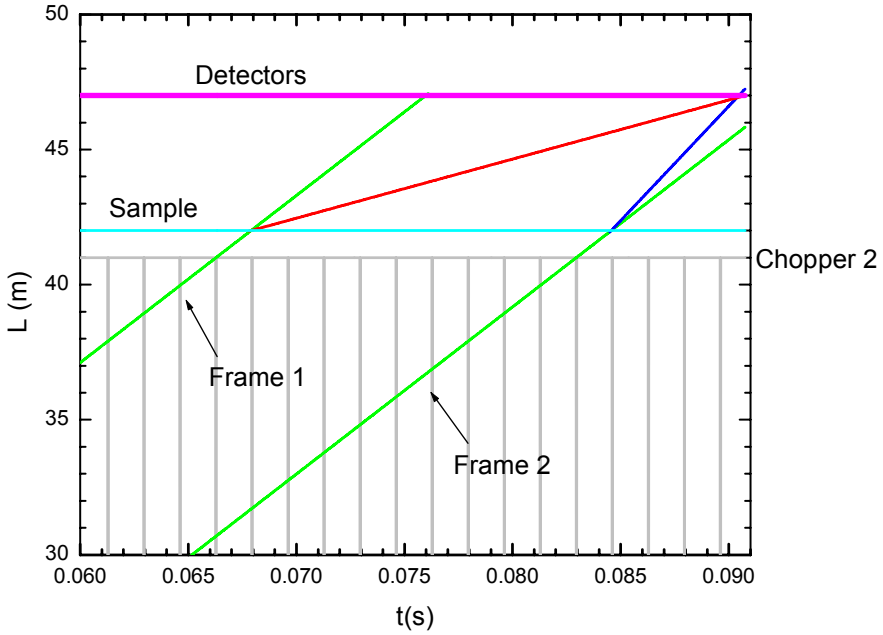

Figure 13 A closer view of the secondary spectrometer region of the timing diagram shown in Figure 12, particularly highlighting the frame overlap problem.

Basically, the neutron energy gain scattering from frame 2 interferes with the desired neutron energy loss scattering from frame 1. In order to solve this problem for these low energy cases, the order suppression chopper must also be able to run at 30 Hz. The net result is shown in Figure 14.

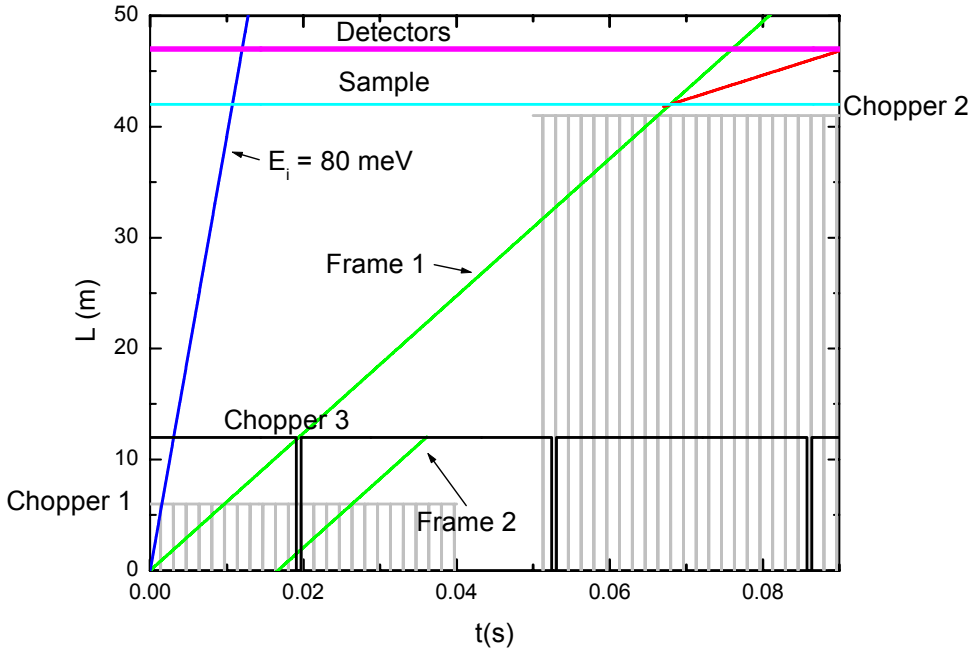

Figure 14 Timing diagram showing the 30 Hz mode for the frame overlap chopper.

Alternatively if the neutron energy gain scatter is the desired quantity to measure, the 30 Hz frame overlap chopper can be phased to be open for frame 2. Then counting over the latter portion of frame 1 will provide neutron energy gain.

2.2.4 Detector Design

The detector bank design has been chosen to provide the maximum Q coverage in the horizontal scattering plane and the ability to examine regions out of the horizontal plane. Because of their high detection efficiency, banks of ^{3}He tubes will be used. Specifically, tubes with PSD capability are chosen to make the instrument well suited to single crystal studies.

For the studies requiring the finest resolutions, the geometrical factors of the detector can contribute to the energy resolution of the spectrometer. One contribution arises from the average depth into the detector that the neutron travels before detection (penetration depth). However, the primary contribution arises from the cylindrical shape

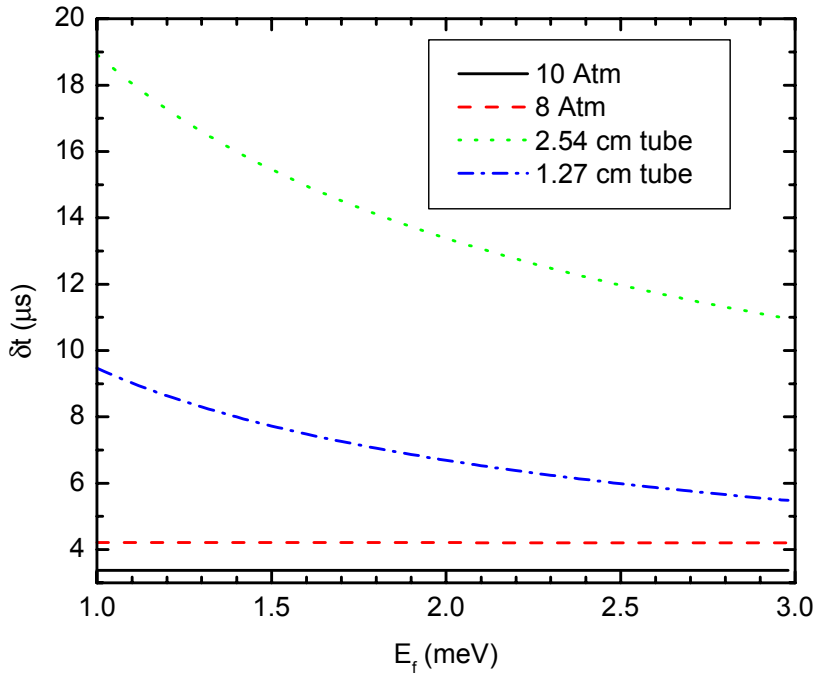

Figure 15 The timing resolution contribution from the penetration depth into the tube for tubes of various pressures and the contribution from the shape of 2.54 cm and 1.27 cm tubes.

of the detector. A simple argument shows that the shape contribution is dominant. For E_i < 5 meV the penetration depth into the detector is on the order of millimeters and the average distance traveled to different points on the tube is on the order of cm. Since energy is related to distance by the square of the distance traveled, there is a significant difference in how these two contributions affect the energy resolution. A more complete analysis of the resultant timing resolution is shown in Figure 15. The curves labeled 8 and 10 Atm show the contribution to the timing uncertainty from the penetration depth

into tubes filled to a pressure of 8 and 10 Atm respectively. The other two curves label the geometrical contributions from tubes of 2.54 cm in diameter and tubes of 1.27 cm in diameter. Notice that the curves related to the penetration depth make a negligible contribution to the timing resolution when compared to the curves related to shape of the detector. Therefore tubes with P = 8 Atm of ^{3}He will be used.

Figure 15 also shows that there is a significant difference in timing uncertainty between the 2.54 cm and 1.27 cm tube. Since using 1.27 cm tubes more than doubles the cost of the detectors, a careful analysis of how these timing resolution contributions affect the overall instrument resolution has been preformed. Figure 16 shows the results of

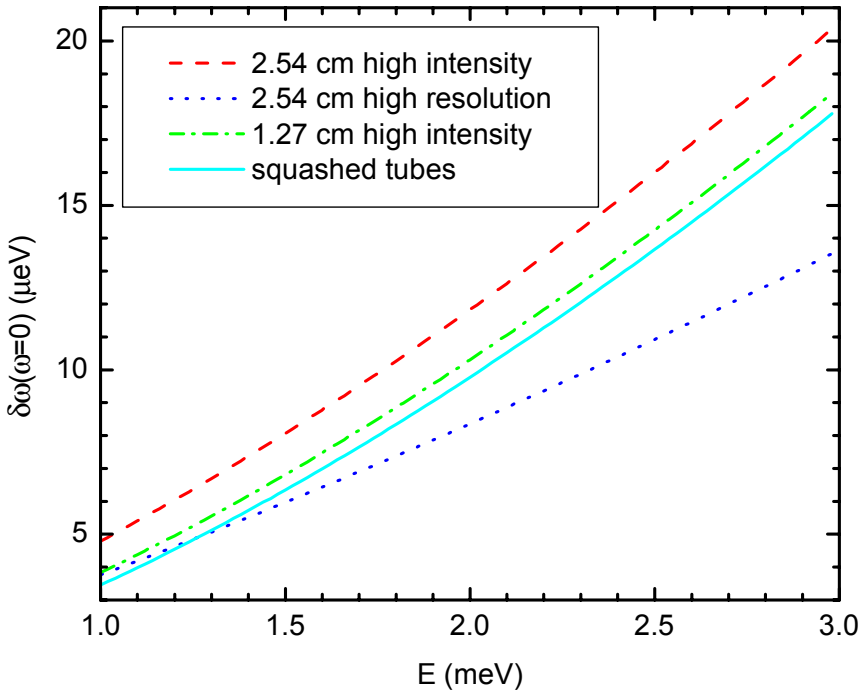

Figure 16 Elastic energy resolution for different diameter ^{3}He tubes and squashed tubes.

including the timing contribution from Figure 15 in the 3rd term in Equation (1). When this contribution is added, the elastic energy resolution at E = 2 meV is 11.8 μeV instead of 10 μeV for the 2.54 cm detectors with the spectrometer operating in the high intensity mode. However, 10 μeV resolution is achieved in the high resolution mode. Moving to 1.27 cm detectors does provide an improvement, but a finer δω of ~1.8 μeV in the high intensity mode does not justify more than doubling the cost of the detector bank. Finally the situation is shown for 8 Atm squashed detectors in the high intensity mode. PSD versions of these squashed detectors are not currently available, however it would probably be a relatively small step in technology to develop them. Their cost would be approximately the same as the 2.54 cm cylindrical detectors making such a detector the ideal choice for this instrument.

These arguments also provide additional reasons that the crystal monochromator-Fermi chopper instrument with a shorter final flight path is not a more optimal instrument. The effects described above are more pronounced for shorter flight paths. Therefore squashed detectors would be a requirement not a luxury for such an instrument and they currently do not exist.

2.3 Performance Details

This section will fill in the remaining details of instrument performance. An extended discussion of the Q resolution and an intensity comparison to other instruments will be provided. Aspects of the energy resolution have been discussed in great detail in Sections 2.1 and 2.2.4, therefore the discussion will not be repeated here.

2.3.1 Momentum transfer resolution

In a similar manner to the energy resolution, the resolution of the momentum transfer (Q) can be quantified by calculations originally designed for a single chopper instrument, with the moderator time width replaced by the time width produced by chopper 1. From the work of Carpenter *et al*[6]., the Q resolution is given by the following equations

$$\delta Q_x = \frac{m_n}{\hbar}\left[\begin{array}{l}\frac{1}{L_1^2}\left(v_i^2 + v_f^2\frac{L_2}{L_3}\cos(\varphi)\right)^2\delta t_p^2 + \frac{1}{L_1^2}\left(v_i^2 + v_f^2\frac{L_1+L_2}{L_3}\cos(\varphi)\right)^2\left(\tau_c + \frac{\delta\alpha^2}{\omega^2}\right) + \\ \left(\frac{v_f^2}{L_3}\cos(\varphi)\right)^2\delta t_m^2 + \left(v_f\sin(\varphi)\right)^2\delta\varphi^2\end{array}\right]^{\frac{1}{2}} \quad (6)$$

$$\delta Q_y = \frac{m_n}{\hbar}\left[\begin{array}{l}\left(\frac{v_f^2 L_2}{L_1 L_3}\sin(\varphi)\right)^2\delta t_p^2 + \left(\frac{v_f^2}{L_1}\frac{L_1+L_2}{L_3}\sin(\varphi)\right)^2\tau_c^2 + \left(\frac{v_f^2}{L_3}\sin(\varphi)\right)^2\delta t_m^2 + \\ \left(v_f\cos(\varphi)\right)^2\delta\varphi^2 + \left(v_i + \frac{v_f^2}{L_1\omega}\frac{L_1+L_2}{L_3}\sin(\varphi)\right)^2\delta\alpha^2\end{array}\right]^{\frac{1}{2}} \quad (7)$$

$$\delta Q = \frac{2}{Q}\sqrt{Q_x^2\delta Q_x^2 + Q_y^2\delta Q_y^2} \quad (8)$$

$$\tau_c = \frac{d}{2\omega r}, \quad (9)$$

where Q_x and Q_y are the components of the momentum transfer parallel and perpendicular to the incident beam respectively, ϕ is the angle between these two components, δQ_x and δQ_y are their uncertainties, the distance parameters L_1, L_2, and L_3 are given in Figure 5, ω is the angular frequency of the second chopper, d is the aperture of that chopper, r is the radius of that chopper, and $\delta\alpha$ is the horizontal divergence at the sample. The only quantity in Equations (6)-(9) that is not simply calculated is $\delta\alpha$.

Therefore, a plot showing the intensity of neutrons with horizontal divergence $\delta\alpha$ as a function of E_i was calculated using the Mcstas Monte Carlo routines[10] and is shown in Figure 17. For $E_i < 70$ meV the intensity is uniform over a broad range of divergences. Therefore, the intensity vs. $\delta\alpha$ was fit to a square function for each energy and the resultant FWHM as a function of energy are plotted in Figure 18. Since 2.54 cm detectors placed on a 5 m radius have an angular uncertainty of ~0.3°, clearly the divergence on the sample is the primary contributor to the Q resolution. Therefore, collimation is required to obtain the highest Q resolution.

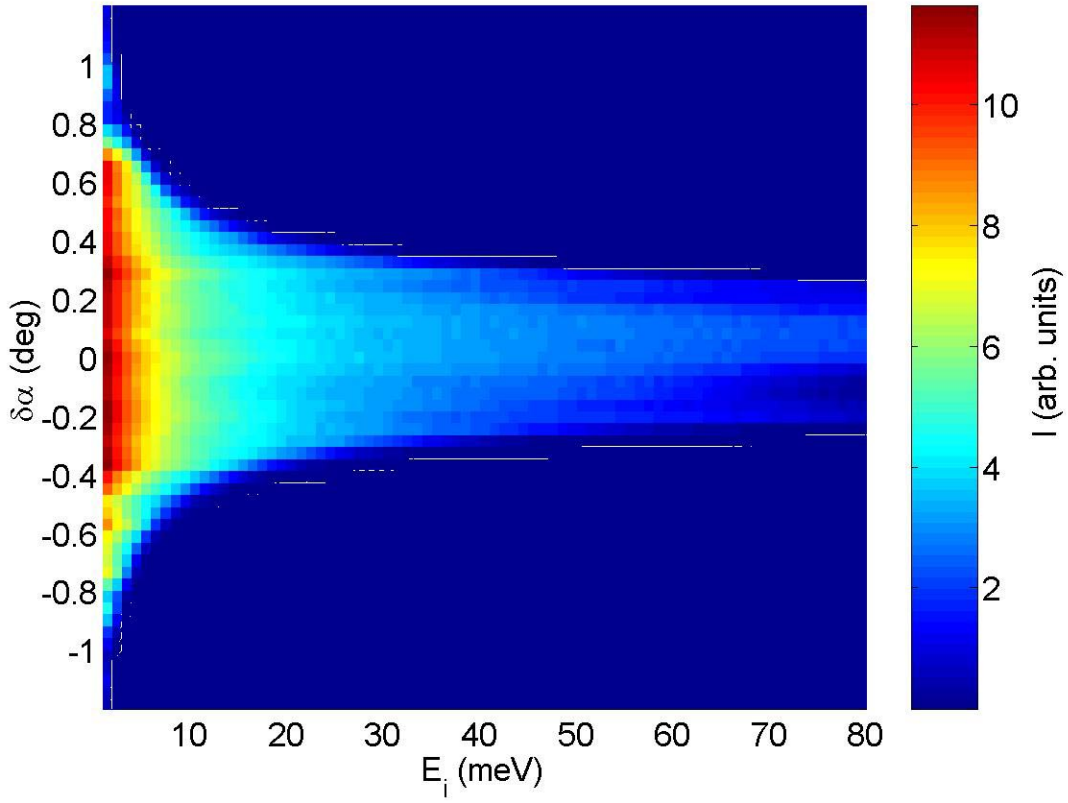

Figure 17 Intensity for different divergences vs. incident energy

Now to examine the elastic Q resolution of the Multichopper instrument, the results from Figure 18 were plugged into Equations (6)-(9) for several angles. The results are shown in Figure 19 and, for comparison, results for $\delta\alpha = 30'$ are shown as well. Notice that for most detector angles the design criterion of $\delta Q < 0.02$ is met at the smallest Q's. Also notice that the introduction of a 30' collimator allows this limit to easily be obtained for a broad range of Q's. Therefore a small set of collimators will be required to fulfill the design constraints. Also, a small segment of diverging guide could be used for similar purposes with larger samples.

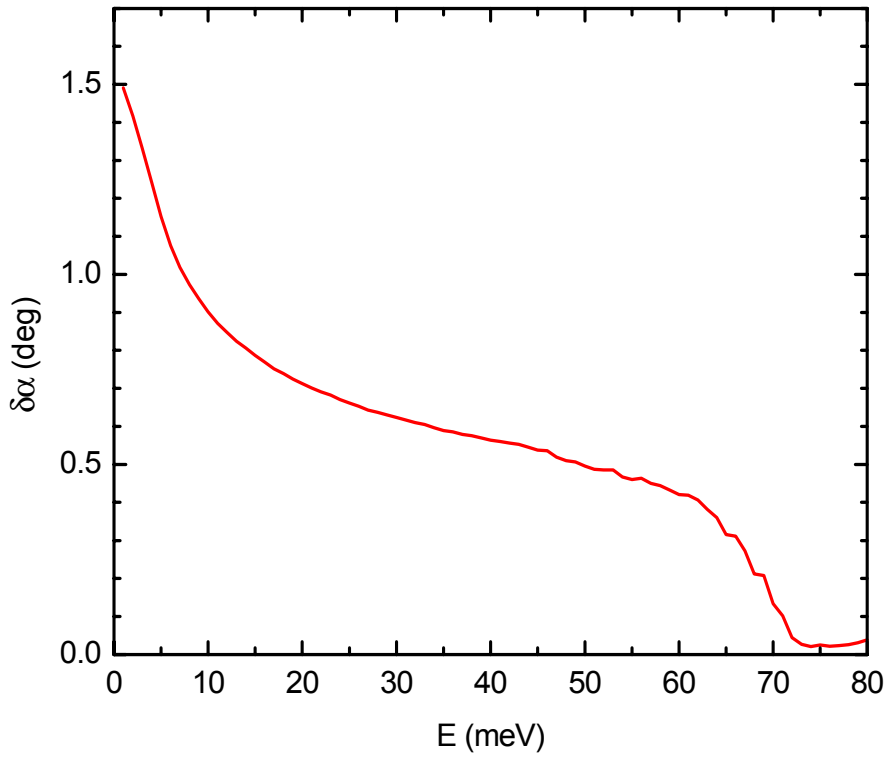

Figure 18 The horizontal divergence at the sample position as provided by the guide system.

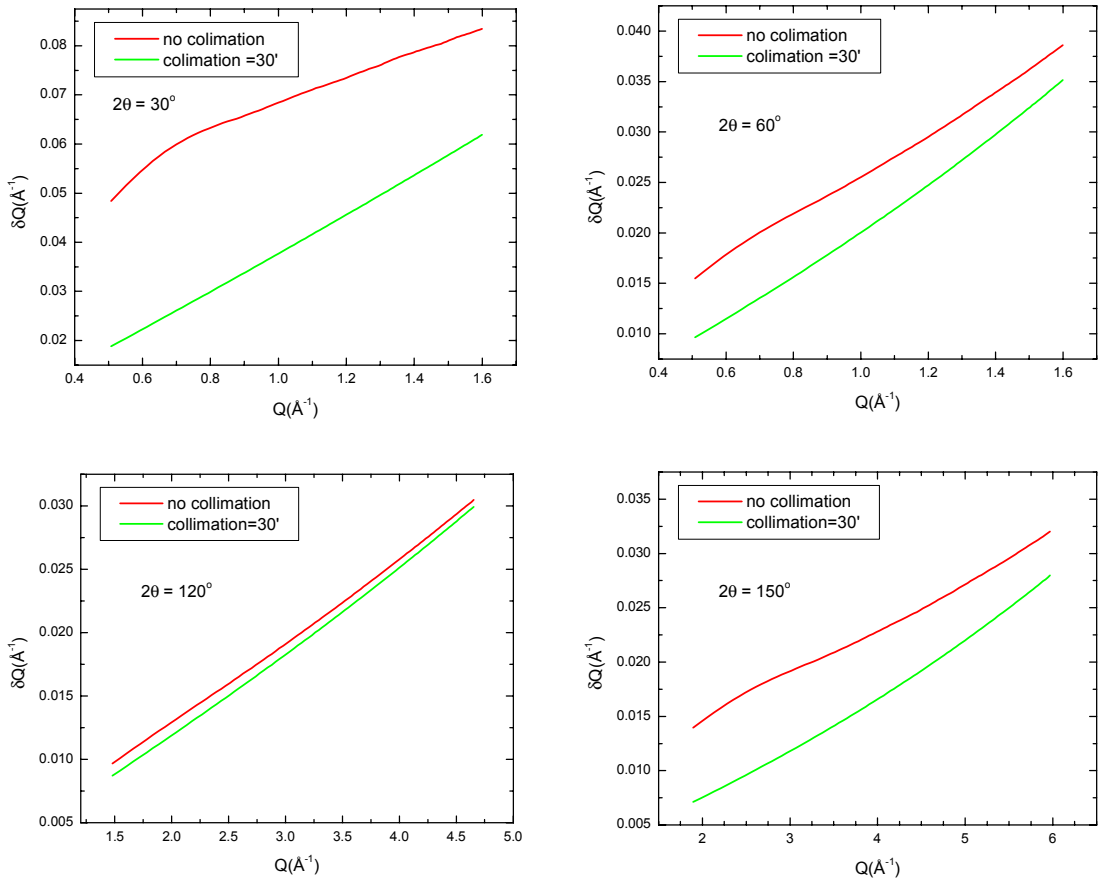

Figure 19 Q resolution as a function of Q for several different angles. Cases where the divergence on sample has values of those shown in Figure 18 and 30' are plotted.

2.3.2 Intensity comparison

Figure 3 shows the flux of neutrons at the sample position for the Multichopper spectrometer as a function of resolution and ω. Comparisons with other disc chopper instruments are summarized in Table 3. This table shows that for equivalent resolutions, the Multichopper instrument will have two orders of magnitude more flux at the sample position than existing instruments. Another appropriate comparison is to the cold triple axis SPINS located at NIST[12]. It produces $4x10^6$ n/cm^2/s on sample at an $E_i \sim 5$meV. Roughly speaking, the Multichopper instrument will have the same flux on sample as SPINS. However with the large detector bank and use of time of flight to measure final energy, the data rate will be significantly higher when mapping large ranges of Q-ω space.

Table 3 Flux on sample for several Disc chopper instruments

Spectrometer	$n/cm^2/s$ ($E_i \sim 5$ meV $\delta\omega \sim 100$ μev)
IN5[3] (ILL)	7×10^4
NEAT[4] (HMI)	2×10^4
DCS[5] (NIST)	2×10^4
Multichopper at SNS	6×10^6

3 Work in Progress

There are several aspects of study that are still in progress. The major one is finding a guide configuration with the gain of the configuration shown here up to 60-80 meV, but several orders of magnitude down for energies above 80 meV. This is needed because the choppers are less efficient at blocking neutrons of E > 80 meV. These neutrons will produce a significant background contribution and, as discussed in Section 2.2.3, the distance between chopper 3 and chopper 1 is controlled by the guide cutoff for the fast neutrons. Preliminary results from ballistic guides with sharp kinks look promising, however more work is required.

Another point under study is squashed ^{3}He PSD detectors. As described in Section 2.2.4, the ability to remove the detector contribution from the energy resolution for little additional cost would benefit this instrument. The French company Eurisys Mesures, that has expertise in squashed detectors but not in the wires to make them position sensitive, is looking into the possibility of fabricating squashed position sensitive detectors.

References

[1] IOC Report of August 24,1999
[2] Magnetism working group report, SNS document number ES-1.1.8.4-8001-MM-A-00; inelastic scattering workshop report, SNS document number IS-1.1.8.2-8004-MM-A-00
[3] http://www.ill.fr/YellowBook/IN5/EDIT94/IN5tab.gif
[4] http://www.hmi.de/bensc/instrumentation/instrumente/v3/v3.html
[5] J. D. Copley, Private communications; http://www.ncnr.nist.gov/instruments/dcs/
[6] J. Carpenter *et al*., Argonne National Laboratory, Report ANL-78-88 (1978)
[7] C. J. Carlile *et al*., in "Neutron scattering in the Nineties", (1985)
[8] http://www.ill.fr/YellowBook/IN6/
[9] http://www1.psi.ch/www_sinq_hn/SINQ/instr/FOCUS.html
[10] K. Neilsen and K. Lefmann, RISØ Document number Risø-R-1175(EN) (2000)
[11] K. W. Herwig, SNS Document numberES-1.1.8.4-6017-RE-A-00
[12] http://www.ncnr.nist.gov/spins.html